HHS Public Access

Author manuscript

Proc SPIE Int Soc Opt Eng. Author manuscript; available in PMC 2018 September 13.

Published in final edited form as:

Proc SPIE Int Soc Opt Eng. 2018 ; 10497: . doi:10.1117/12.2290631.

Quantifying cancer cell receptors with paired-agent fluorescent imaging: a novel method to account for tissue optical property effects

Negar Sadeghipour[a], **Scott C. Davis**[b], and **Kenneth M. Tichauer**[a]

[a]Department of Biomedical Engineering, Illinois Institute of Technology, 3255 S Dearborn St., Chicago, IL USA 60616

[b]Thayer School of Engineering, Dartmouth College, 14 Engineering Dr., Hanover, NH USA 03755-8001

Abstract

Dynamic fluorescence imaging approaches can be used to estimate the concentration of cell surface receptors *in vivo*. Kinetic models are used to generate the final estimation by taking the targeted imaging agent concentration as a function of time. However, tissue absorption and scattering properties cause the final readout signal to be on a different scale than the real fluorescent agent concentration. In paired-agent imaging approaches, simultaneous injection of a suitable control imaging agent with a targeted one can account for non-specific uptake and retention of the targeted agent. Additionally, the signal from the control agent can be a normalizing factor to correct for tissue optical property differences. In this study, the kinetic model used for paired-agent imaging analysis (i.e., simplified reference tissue model) is modified and tested in simulation and experimental data in a way that accounts for the scaling correction within the kinetic model fit to the data to ultimately extract an estimate of the targeted biomarker concentration.

Keywords

Dynamic fluorescence imaging; kinetic modeling; Epidermal growth factor receptor quantification

1. INTRODUCTION

In cancer therapy, characterizing different types of biomarkers is a key component in identifying patients who are likely to respond to a given therapy.[1] Moving away from measuring these biomarkers from tumor biopsies and toward more non-invasive methods such as imaging techniques should allow better monitoring of oncology patients.[2,3] In fluorescence imaging, syntheses of new targeted imaging agents are rapidly expanding.[4,5] Despite its limitations in whole-body human imaging, fluorescence imaging is suitable for dynamic small animal "*in vivo*" imaging.[6,7] Cell surface receptors that transmit proliferation signals are important biomarkers in cancer research.[8,9] Mathematical models are needed to

Further author information: (Send correspondence to K.M.T), K.M.T.: ktichauer.iit.edu, Telephone: 1 312 567 3858.

analyze the fluorescence data and to quantify the available cell surface receptors.[10–14] Paired-agent imaging is a successful approach to quantify cell surface receptors *in vivo*.[15,16] In this technique, a second control counterpart of the targeted imaging agent is co-injected with the targeted one to account for non-specific uptake and retention of the targeted imaging agent.[17,18] The control agent is labeled with fluorophore having its emission peak at a different channel than the targeted fluorophore. In this way, the two imaging agents can be imaged at the same time with a spectrally resolved imaging device. Paired-agent imaging has shown promising results in quantifying cell surface receptors.[19,20] However, distorting effects of the optical absorption and scattering of tissue is an obstacle in measuring of fluorescent agent concentrations accurately.[21] These tissue optical property effects could cause errors in paired-agent imaging, if not accounted for, since the two imaging agents are often imaged at different wavelength that could have different tissue optical properties. As a result, a normalization tool must be applied to correct for tissue optical property differences. In the previous study,[22] a pixel-by-pixel normalization tool was demonstrated to partially account for spatial variability in the optical property differences by dividing the targeted signal to the control signal at a 1-minute post-injection time point. In this method it is assumed that an early time point data after injection is available and the targeted and control signals are affected only by the tissue optical properties at early time points after imaging agent administration.[22] Correcting for optical tissue properties with a factor in the kinetic model is another way of normalizing for tissue attenuation between the two imaging agents.

In this study, the dynamic simplified reference tissue kinetic model that is applied to the paired-agent imaging methods is compared in two different cases: 1) as it was originally used by taking the pixel-by-pixel normalized targeted and control curves for its inputs and 2) as a modified version by taking the intact signals directly to the model. The models were evaluated in simulation and in a subcutaneous tumor mouse study.

2. METHODS AND RESULTS

2.1 Animal Experiment

The detailed animal model study can be found here.[23] Briefly, a group (n = 6) of athymic nude mice were injected subcutaneously with A431 tumor, known for a high level of epidermal growth factor receptor (EGFR) overexpression. After the tumors got to the appropriate size (about 5 mm in diameter), the skin above the tumors was removed, and the mice were injected intravenously with a cocktail of IRDye 800CW-EGF (targeted) and IRDye 700DX-carboxylate (control) (0.2 nanomoles each). Mice were immediately placed in a two-channel (700 and 800 nm) Odyssey (LICOR Biosciences, Lincoln, NE) scanner and fluorescent images at 700–740 nm (excitation: 685 nm) and 800–840 nm (excitation: 785 nm) were acquired every two minutes for 1 h. The data were later corrected by normalizing each image stack with a pixel-by-pixel normalization factor (the details of this approach can be found in[22]). The corrected data were evaluated by the original simplified reference tissue model (O-SRTM) explained in 2.3.1. Moreover, the raw data were given inputed to the modified SRTM (M-SRTM) as explained in section 2.3.2.

Figure 1 is the results of BP estimation by the two methods. A strong correlation was observed between M-SRTM and O-SRTM measures of binding potential for A431 cell line,

in vivo (r=0.79, slope=.79, and intercept=0.40). In all of this, it is assumed the uptake of the two imaging agents are similar in the blood plasma, however, this assumption needs to be tested in future work.[24]

2.2 Simulation

A simulation study was carried out by creating targeted and control imaging agent concentration curves from an experimentally-derived plasma input curve of EGF molecule. The data is solved through a standard Kety model.[25] After giving artificial scales to the targeted curves (to simulate the scale differences), the created curves were given 1000 times noise iterations and they were fitted into the O-SRTM and M-SRTM. Figure 2 (a) and (b) are showing an example of the created curves without noise and after adding Poisson noise and scaling the targeted curves, respectively. Figure 2 (c) is Relative error in BP estimation after increasing the time of normalization from 1 minutes to 10 minutes post tracers injection. According to this plot the underestimaton of BP increases by increasing the pixel-by-pixel normalization time.

In Figure 3, the results of O-SRTM and M-SRTM parameter estimation, for different given scaling factors are shown. According to this figure, both models are pretty stable in BP estimation regardless of the given scaling factor. O-SRTM is underestimating the BP for about 2.5% and M-SRTM is overestimating it for about 5%. The underestimation of BP by O-SRTM will increase by increasing the time of normalization from 1 minute post-injection. O-SRTM underestimates the k_2 and R_1 parameters while M-SRTM overestimate the k_2 and underestimate a.

2.3 Paired-agent Kinetic Model

Paired-agent kinetic models are based on a two-tissue and one-tissue compartment models. Schematic details of the model is shown in Figure 4. The goal of the model is to estimate the binding potential (BP), a parameter proportional to cell surface receptor concentration.

2.3.1 Original Reference Tissue Model (O-SRTM)—Quantification of EGFR was determined using a least square curve fit model in Matlab R2016a. The kinetic model is developed and adopted from a simplified reference tissue model originally introduced for PET imaging.[26] The model is shown in equation (1)

$$ROI_T = \frac{\eta_T}{\eta_C}[R_1 ROI_C + k_2(1 - \frac{R_1}{1+BP})e^{-\frac{k_2}{1+BP}t} * ROI_C], \quad (1)$$

where, ROI_T and ROI_C are detected targeted and control agent signals measured in a region of interest, respectively. η_T and η_C are correction factors relating detected targeted and control agent signals to corresponding agent concentration. R_1 is the ratio of extravasation of the targeted to the control agent. k_2 is the efflux rate constant, BP is the binding potential, t is the time and * is convolution.

In pixel-by-pixel paired-agent imaging approaches, the η_T/η_C ratio was considered to be 1. As a result, the final number of fitting parameters in O-SRTM is reduced to 3 parameters R_1, k_2, and BP.

2.3.2 Modified Reference Tissue Model (M-SRTM)—The modified SRTM, M-SRTM, is introduced in equation (2). In this model the new parameter of α_{tumor} is introduce to the model for the $\frac{\eta_T}{\eta_C}$. This means a new fitting parameter is added to the model, however, by keeping R_1 close to 1, by choosing imaging agents that have similar rate of extravasation from blood flow, as a result, the final fitting parameters are α_{tumor}, k_2 and BP.

$$ROI_T = \alpha_{tumor} ROI_C + \alpha_{tumor} k_2 (1 - \frac{1}{1+BP}) ROI_C * e^{-\frac{k_2}{1+BP}t}, \quad (2)$$

Acknowledgments

This work was sponsored by NIH research grant R01 CA184354, NSF CAREER 1653627, and the Nayar Prize at Illinois Institute of Technology. We would also like to acknowledge Prof Brian W Pogue and Prof Kimberley S Samkoe of Dartmouth College for sharing the animal data used in the analysis here.

References

1. Kelloff GJ, Sigman CC. Cancer biomarkers: selecting the right drug for the right patient. Nature reviews Drug discovery. 2012; 11(3):201–214. [PubMed: 22322254]
2. Weissleder R. Molecular imaging in cancer. Science. 2006; 312(5777):1168–1171. [PubMed: 16728630]
3. Weissleder R, Pittet MJ. Imaging in the era of molecular oncology. Nature. 2008; 452(7187):580–589. [PubMed: 18385732]
4. Kobayashi H, Ogawa M, Alford R, Choyke PL, Urano Y. New strategies for fluorescent probe design in medical diagnostic imaging. Chemical reviews. 2009; 110(5):2620–2640.
5. Rao J, Dragulescu-Andrasi A, Yao H. Fluorescence imaging in vivo: recent advances. Current opinion in biotechnology. 2007; 18(1):17–25. [PubMed: 17234399]
6. Davis SC, Samkoe KS, Tichauer KM, Sexton KJ, Gunn JR, Deharvengt SJ, Hasan T, Pogue BW. Dynamic dual-tracer mri-guided fluorescence tomography to quantify receptor density in vivo. Proceedings of the National Academy of Sciences. 2013; 110(22):9025–9030.
7. Koo V, Hamilton P, Williamson K. Non-invasive in vivo imaging in small animal research. Analytical Cellular Pathology. 2006; 28(4):127–139.
8. Stangl S, Gehrmann M, Dressel R, Alves F, Dullin C, Themelis G, Ntziachristos V, Staeblein E, Walch A, Winkelmann I, et al. In vivo imaging of ct26 mouse tumours by using cmhsp70. 1 monoclonal antibody. Journal of cellular and molecular medicine. 2011; 15(4):874–887. [PubMed: 20406322]
9. Carson-Walter EB, Watkins DN, Nanda A, Vogelstein B, Kinzler KW, Croix BS. Cell surface tumor endothelial markers are conserved in mice and humans. Cancer research. 2001; 61(18):6649–6655. [PubMed: 11559528]
10. Fibich G, Hammer A, Gannot G, Gandjbakhche A, Gannot I. Modeling and simulations of the pharmacokinetics of fluorophore conjugated antibodies in tumor vicinity for the optimization of fluorescence-based optical imaging. Lasers in surgery and medicine. 2005; 37(2):155–160. [PubMed: 16037970]

11. Stein AM, Demuth T, Mobley D, Berens M, Sander LM. A mathematical model of glioblastoma tumor spheroid invasion in a three-dimensional in vitro experiment. Biophysical journal. 2007; 92(1):356–365. [PubMed: 17040992]
12. Dai X, Chen Z, Tian J. Performance evaluation of kinetic parameter estimation methods in dynamic fdg-pet studies. Nuclear medicine communications. 2011; 32(1):4–16. [PubMed: 21166088]
13. Salinas C, Weinzimmer D, Searle G, Labaree D, Ropchan J, Huang Y, Rabiner EA, Carson RE, Gunn RN. Kinetic analysis of drug–target interactions with pet for characterization of pharmacological hysteresis. Journal of Cerebral Blood Flow & Metabolism. 2013; 33(5):700–707. [PubMed: 23385202]
14. Xu X, Wang Y, Xiang J, Liu JTC, Tichauer KM. Rinsing paired-agent model (rpam) to quantify cell-surface receptor concentrations in topical staining applications of thick tissues. Physics in medicine and biology. 2017; 62(12):5098. [PubMed: 28548970]
15. Sadeghipour N, Davis S, Tichauer K. Generalized paired-agent kinetic model for in vivo quantification of cancer cell-surface receptors under receptor saturation conditions. Physics in medicine and biology. 2016; 62(2):394. [PubMed: 27997381]
16. Tichauer KM, Samkoe KS, Sexton KJ, Gunn JR, Hasan T, Pogue BW. Improved tumor contrast achieved by single time point dual-reporter fluorescence imaging. Journal of biomedical optics. 2012; 17(6):0660011–06600110.
17. Samkoe KS, Tichauer KM, Gunn JR, Wells WA, Hasan T, Pogue BW. Quantitative in vivo immunohistochemistry of epidermal growth factor receptor using a receptor concentration imaging approach. Cancer research. 2014; 74(24):7465–7474. [PubMed: 25344226]
18. Liu JT, Helms MW, Mandella MJ, Crawford JM, Kino GS, Contag CH. Quantifying cell-surface biomarker expression in thick tissues with ratiometric three-dimensional microscopy. Biophysical journal. 2009; 96(6):2405–2414. [PubMed: 19289065]
19. Tichauer K, Samkoe K, Klubben W, Hasan T, Pogue B. Advantages of a dual-tracer model over reference tissue models for binding potential measurement in tumors. Physics in medicine and biology. 2012; 57(20):6647. [PubMed: 23022732]
20. Tichauer KM, Wang Y, Pogue BW, Liu JT. Quantitative in vivo cell-surface receptor imaging in oncology: kinetic modeling and paired-agent principles from nuclear medicine and optical imaging. Physics in medicine and biology. 2015; 60(14):R239. [PubMed: 26134619]
21. Kim A, Khurana M, Moriyama Y, Wilson BC. Quantification of in vivo fluorescence decoupled from the effects of tissue optical properties using fiber-optic spectroscopy measurements. Journal of biomedical optics. 2010; 15(6):067006–067006. [PubMed: 21198210]
22. Kanick SC, Tichauer KM, Gunn J, Samkoe KS, Pogue BW. Pixel-based absorption correction for dual-tracer fluorescence imaging of receptor binding potential. Biomedical optics express. 2014; 5(10):3280–3291. [PubMed: 25360349]
23. Tichauer KM, Samkoe KS, Sexton KJ, Hextrum SK, Yang HH, Klubben WS, Gunn JR, Hasan T, Pogue BW. In vivo quantification of tumor receptor binding potential with dual-reporter molecular imaging. Molecular Imaging and Biology. 2012; 14(5):584–592. [PubMed: 22203241]
24. Tichauer K, Diop M, Elliott J, Samkoe K, Hasan T, Lawrence KS, Pogue B. Accounting for pharmacokinetic differences in dual-tracer receptor density imaging. Physics in medicine and biology. 2014; 59(10):2341. [PubMed: 24743262]
25. Kety SS. The theory and applications of the exchange of inert gas at the lungs and tissues. Pharmacological reviews. 1951; 3(1):1–41. [PubMed: 14833874]
26. Lammertsma AA, Hume SP. Simplified reference tissue model for pet receptor studies. Neuroimage. 1996; 4(3):153–158. [PubMed: 9345505]

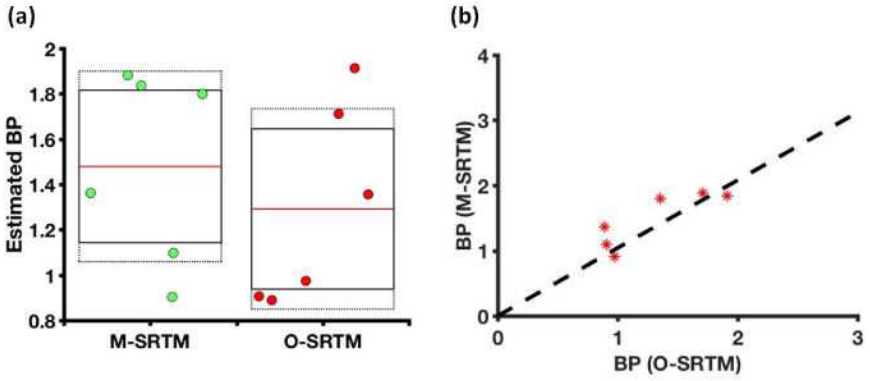

Figure 1.

Experimental results. (a) Estimated BP for A431 tumors, green:M-SRTM and red: O-SRTM. (b) Estimated BP for M-SRTM vs. O-SRTM.

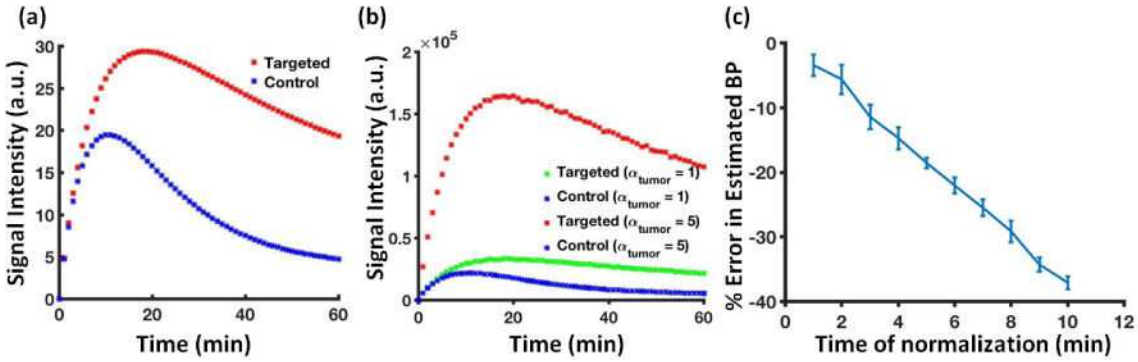

Figure 2.

(a) simulated targeted and control curves. (b) simulated noise added targeted and control curves with different α_{tumor} (c) % error in BP estimation by O-SRTM method.

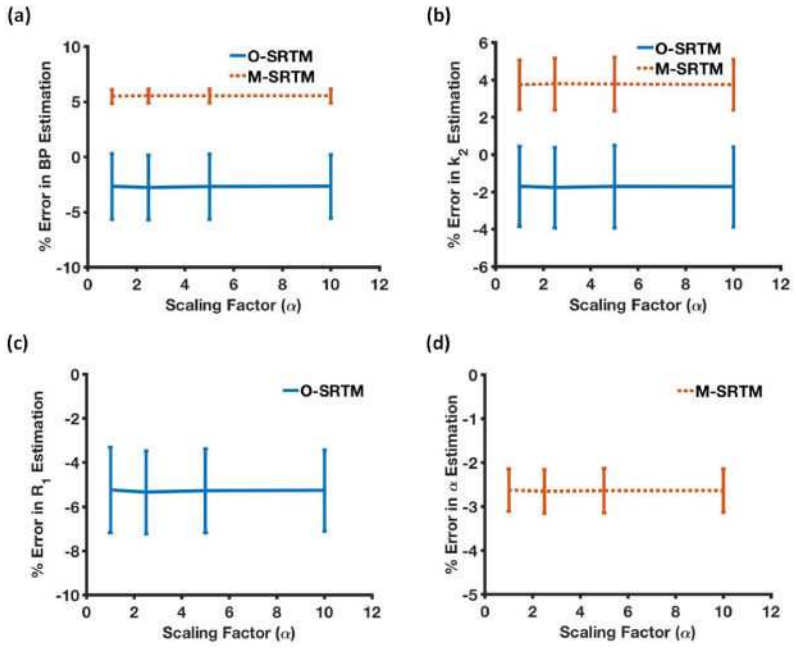

Figure 3.

% of relative errors in estimation of parameters by two kinetic models blue lines: O-SRTM and orange lines: M-SRTM by changing the scaling parameter (α). (a) BP estimation. (b) k_2 estimation. (c) R_1 estimation. (d) α_{tumor} estimation.

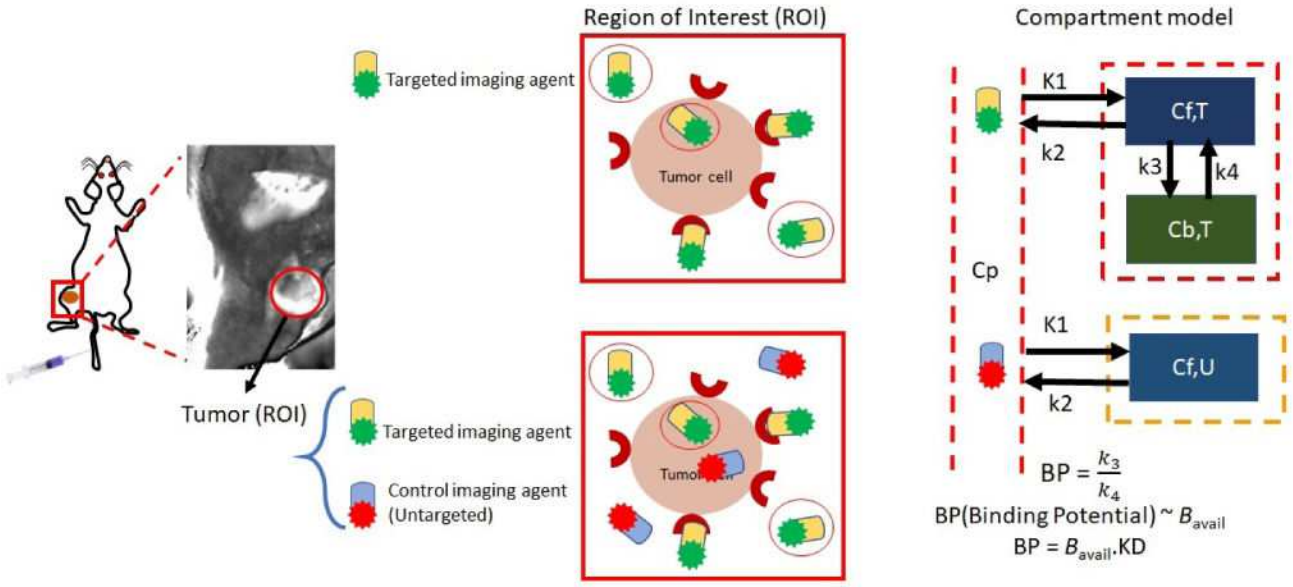

Figure 4.

On the left is a schematic of subcutaneous mouse tumor model is represented. In the middle is an illustration of single targeted imaging agent (top) and how non-specific retention can happen on the surface of a cell or in free space, and the paired-agent imaging methods (bottom) and how it is accounted for the non-specific uptake by a control imaging agent is shown. On the right, compartment models for both the targeted and control tracers are depicted on top and bottom, respectively. K_1 and k_2 represent transit rates of the tracers from the blood plasma, to the extravascular space and back; k_3 and k_4 represent association and dissociation rates of the targeted tracers. Binding potential (BP), is a parameter proportional to the receptor concentration (B_{avail}). K_D is the dissociation rate constant that relates the BP to B_{avail}.